Evaluation of EDXRF configurations to improve the limit of detection and exposure for *in vivo* quantification of gadolinium in tumor tissue

M. Santibáñez, M. Vásquez, R.G. Figueroa, M. Valente

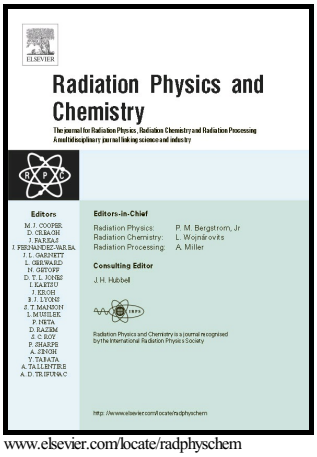

www.elsevier.com/locate/radphyschem

PII: S0969-806X(16)30015-9
DOI: http://dx.doi.org/10.1016/j.radphyschem.2016.01.015
Reference: RPC7029

To appear in: *Radiation Physics and Chemistry*

Received date: 8 October 2015
Revised date: 2 December 2015
Accepted date: 12 January 2016

Cite this article as: M. Santibáñez, M. Vásquez, R.G. Figueroa and M. Valente Evaluation of EDXRF configurations to improve the limit of detection an exposure for *in vivo* quantification of gadolinium in tumor tissue, *Radiatio Physics and Chemistry,* http://dx.doi.org/10.1016/j.radphyschem.2016.01.015

Evaluation of EDXRF configurations to improve the limit of detection and exposure for *in vivo* quantification of gadolinium in tumor tissue

M. Santibáñez[1*], M. Vásquez[1] R.G. Figueroa[1] and M. Valente[1,2]

[1] Departamento de Ciencias Físicas, Universidad de la Frontera, Avda. Francisco Salazar 01145, Temuco, Chile.
[2] Institute of Physics E. Gaviola - CONICET LIIFAMIR[x] - University of Córdoba, Ciudad Universitaria, 5000 Cordoba, Argentina.

*E-mail: mauricio.santibanez@ufrontera.cl

Abstract.

In this paper the configuration of an Energy Dispersive X-Ray Fluorescence (EDXRF) system optimized for *in vivo* quantification of gadolinium in tumor tissue was studied. The system was configured using XMI-MSIM software designed to predict the XRF spectral response using Monte Carlo simulations. The studied setup is comprised of an X-ray tube, tuned to different voltages, and a copper filter system configured with variable thickness, which emits a spectrally narrow beam centered on the specific excitation energy. The values for the central energy excitation and the spectral width were adjusted to optimize the system, using like figures of merit: minimization of the limit of detection, measurement uncertainty and radiation exposure. These values were obtained in two stages. The first was successive simulations of incident spectra with central energy in the range of 50-70 keV. The second was comprised of simulations with incident spectra of different widths (8-29 keV), all with the same determined central energy, evaluating the limit of detection depending on the exposure. This made it possible to find the best balance between system sensitivity and the delivered dose. The obtained results were compared with those produced by radioactive sources of ^{241}Am whose activity was set to produce the same exposure as the proposed setup. To evaluate the feasibility of *in vivo* quantification, a set of tumor phantoms of 1-6 cm^3 at different depths and labeled with a gadolinium concentration of 250 ppm was evaluated. From the resulting spectrum, calibration curves were obtained in function of the size and depth of the tumor, allowing for the evaluation of the potential of the methodology.

Keywords: Gadolinium, *in vivo* EDXRF, XMI-MSIM.

1. Introduction

Gadolinium (Gd) is an element that has been widely used as an examination contrast medium, mainly in brain magnetic resonance imaging (MRI) (Le and Cui, 2006; Fujimoto et al., 2009). In the last decades Gd has begun to be applied in neutron capture therapy (NCT) due to high cross section for thermal neutrons. It produces Auger electrons, internal conversion electrons, Gamma-prompt rays and X-rays and releases approximately 7.94 MeV (Dewi et al., 2013; Enger et al., 2013; Shih and Brugger; 1999). In order to determine the dose of radiation administered to the tumor by this type of therapy, the amount of

Gd present must be known. Therefore it is necessary to quantify its presence in the tissue and how it is distributed within it.

Gd concentration has been studied in the literature using *in vivo* neutron activation analysis (IVNAA). In IVNAA, a ^{238}Pu/Be neutron source is used, which excites Gd nuclei, generating unstable isotopes which release excess energy by Gamma-prompt rays. These are in turn detected, indicating the presence of this element (Gräfe; 2011; Gräfe et al., 2012). Similarly, Gd quantification by X-rays fluorescence (XRF) in phantom brain tumor have been implemented by ^{241}Am sources, using the 59 keV Gamma photons emitted with 35.7% probability per decay (Almalki et al., 2010).

The problems with studies that have been carried out to date are: how to increase the sensitivity of the deployed systems in order to reduce measurement times required and how to reduce the dose of radiation given to the patient, thus allowing the study of the spatial distribution of Gd in the volume of interest. In order to increase sensitivity in EDXRF systems, it is necessary to increase the production of fluorescence photons exciting the sample with energies near to the Gd absorption edge. However, there are no long half-life isotopes that emit with energies close to this edge, thus raising the need to find another source of excitation with which to identify and quantify Gd by EDXRF. Therefore, we propose the study of the configuration of different X-ray tubes in order to produce spectra that are centered on a specific energy that minimizes the sensitivity of the system, using the concepts of limit of detection and uncertainty as figure of merit. These spectra would include a sufficiently narrow spectral width that achieves a balance between the dose released in the procedure and the required measurement time, by means or relative reduction of photons in low energy channel.

This study aims to produce different configurations of incident spectra with a narrow energy distribution, centered at an energy greater than the K absorption edge, produced by a conventional radio-diagnostic X-ray machine (Figueroa et al., 2015). This will be executed by tuning the voltage (kVp) and the addition of copper filters of varying thickness associated with each kVp. The determination of the optimal spectrum involves maximizing the number of incident photons with energies greater than the absorption edge (since it is not a monochromatic spectrum) while maintaining the distribution of photons as close to the absorption edge as possible in order to maximize the fluorescent emission produced (Figueroa et al., 2015). In the second stage, configurations that produce incident spectrums of same central energy (optimal energy determined) but with different FWHM were evaluated to determine the exposure produced to achieve the same limit of detection values (considering the different measurement time required in each configuration), and thus determine the settings which will produce the lowest dose and maximum sensitivity. In order to compare the proposed system with that available in the literature (Almalki et al., 2010), the limit of detection and measurement uncertainty obtained by the optimized system are compared with respect to the isotope source ^{241}Am (long life isotope with energy closer to the K absorption edge), with and without absorption filter, and an activity of the isotope source adjusted to produce the same exposure in the air than the tube. To implement the method in quantitative applications, a study of Gd quantification in tumors of different sizes and for concentrations in the therapeutic range recommended is performed (around 250 ppm) (Salt et al., 2004; De Stasio et al., 1998). Calibration curves for tumor geometries with fixed distances: source-center and source-surface of the tumor are shown and the results discussed.

2. Materials and methods

2.1 Monte Carlo simulation

The identification and quantification in this study was made considering the characteristic fluorescence emission of Gadolinium Kα (42.8 keV). To determine the optimal parameters, Monte Carlo simulations were realized with the open source software XMI-MSIM version 5.0 (Schoonjans et al., 2013; Vincze et al., 1999), specifically optimized to predict the XRF spectral response in EDXRF systems. Some of the advantages offered by this code in comparison with other similar codes are the simulation of the M-lines and cascade effects, fluorescence and Compton escape peaks and pulse pile-up (Schoonjans et al., 2012). Additionally, the software is optimized for operate in variance reduction techniques, facilitating its implementation without higher computational requirement.

The X-ray source can be defined as a series of discrete lines or continuous energy intervals, each with their own energy, intensity, linear polarization, source dimensions and divergence. Another parameters include the geometry of the system: detector position, orientation, crystal composition, collimator and filters in the excitation and detection path, as well as a description of the electronics parameters: gain, zero, Fano factor, electronic noise (Vincze et al., 1993; Vincze et al., 1999; Schoonjans et al., 2013). The software XMI-MSIM simulates the history of individual photons from the position where they hit on the sample with a given direction and energy to the point where they are either absorbed by a sample atom or emerge from the sample. The type of atom with that the interaction occurs, the distance between two consecutive interactions and the type of interaction are randomly chosen using uniform random numbers (Schoonjans et al., 2012; Vincze et al., 1993). If the simulated photon leaves the simulated volume and the current direction of the photon will make it intersect with the detector the final photon energy will be stored by the program in a virtual multichannel analyzer (MCA) memory, corresponds to a situation with an ideal detector (Vincze et al., 1999; Schoonjans et al., 2012). After the simulation, the energy distribution of the photons is corrected by convolution with terms that take into account the effect of the detector window and the dead-layer, as well as the transmission of the detector crystal, the distribution is convolute with the detector response function that takes into account peak broadening, fluorescence and Compton escape peaks, and pulse pile-up (Schoonjans et al., 2012; Vincze et al., 1999).

The simulation arrangements were formed by: X-ray tubes configured with the typical characteristics of a radiology device, consisting of 90kV max, with a tungsten target, a beryllium window to the output beam of 125 μm and a tube current of 100 mA. The detection system implemented was a LE-Ge detector of 20 cm^2 area and 2 cm thick. The detector energy resolution modeled was a FWHM of 173 eV for 5.9 keV and a FWHM of 558 eV for 122 keV. The number of spectral channels was set to 4096 with a detector gain of 0.06 keV/channel and a detector zero of 0.728 keV. The detector response function is included in the database of the software and has been described in previous work by the developers (Vincze et al., 1993; Vincze et al., 1999).

The phantoms studied were formed by a volume of soft tissue of a density of 1.0 g/cm^3, corresponding to the tissue surrounding the tumor with a thickness of 20 cm. Given that the XMI-MSIM code models the samples as a stack of layer, the tumors simulated have a elipsoidal shape of 1 cm of minor diameter and 1-6 cm of major diameter. All the tumors were doped with 250 ppm of gadolinium considering a homogeneous distribution. The distance between the X-ray sources and the surface of the phantom was set at 20 cm, while the distance to the surface of the phantom from the detector remained

fixed at 20 cm. The acquisition time was set at 16 seconds to assess the feasibility of future generation of 2D images of surface scans. A sketch of the proposed setup is shown in the figure 1.

2.2 Data analysis

The statistical figures of merit used for obtain an optimal qualitative and quantitative analysis of fluorescence peaks in order to increase the sensitivity and reduce the radiation doses, were determined by the limit of detection (LoD) and uncertainty criteria in function of the exposure required for achieve these values. The limit of detection is a statistical criterion to diminish the detection of a signal in terms of to the background of a certain measurement. In X-ray spectroscopy, it is utilized to determine the presence of elemental chemical substances, in which the peak or signal is statistically discriminable from its background (Santibañez et all, 2013; Moya-Riffo et al, 2013; Figueroa et al, 2004). The uncertainty of net peak area of a fluorescence signal ΔI_F, it is defined as the relative error of the fluorescence counts associated to determining its value from the total counts and the modeling of background counts, over the number of fluorescence counts obtained. The increased uncertainty may reduce the accuracy of quantitative measurements especially for very lows concentration of the Gadolinium. The most common definitions of these parameters are given by the Eq. 1 and 2 (Van Grieken and Markowicz, 2002; Jenkins et al., 1988).

$$LoD = \frac{3\sqrt{I_{Bgr}}}{I_F} \quad (1)$$

$$\Delta I_F = \frac{\sqrt{I_{Bgr} + I_{total}}}{I_F} \quad (2)$$

where I_{Bgr} is the number of counts of the background, I_{total} the total number of counts measured and I_F is the number of fluorescence counts, obtained after determining the background in the region where the fluorescence signal is detecting and subtracted to the total counts measured.

On the other hand, the exposure χ is defined as "the ratio *dQ* over *dm*, where *dQ* is the absolute value of the total charge of the ions of the same sign produced in air, when all the electrons and positrons released by the photons in the air volume (of mass *dm*), were completely stopped" (ICRU, 1980). In the case of a continuous spectrum, the exposure will depend on: the energy fluency, attenuation and the ionization potential of the medium, being defined by Eq. 3:

$$\chi = \int_{E=0}^{E_{max}} (\mu_{en}/\rho)_{E,air} \left(e/\dot{W}\right)_{air} \Psi'(E) dE \quad (3)$$

Where $(\mu_{en}/\rho)_{E,air}$ corresponds to the of mass absorption coefficient spectrally weighted, in this case air, $(e/W)_{air}$ is the electron work function in air 1/33.97 *C/J*, *E* is expressed in keV and χ is in C/kg.

These parameters were calculated from the output spectrum data, obtained in the different simulations, considering the counts in the specific spectral Region of interest (ROI) of samples with and without Gd, in order to obtain the total counts and the background counts in the ROI and from these values the desired number of fluorescence counts.

2.3 Setup optimization

Two stages of simulations were carried out for determining the optimal incident spectrum. In the first step, several tube voltages (kVp) were configured such that the peak intensity of the emitted spectrum is centered between 50 to 70 keV (from the absorption edge to the maximum kVp of the tube). To accomplish this, copper filters of different thicknesses for each kVp (see Table 1) were added to obtain a non-symmetrical narrow spectrum with a fixed FWHM. In the second step, a new set of copper filters were defined, making it possible to establish a kVp to allow for the generation of a set of spectra concentrated around on a specific energy (see Table 1), but with FWHM in the range of 8 to 29 keV. The resulting spectra for these settings can be seen in Figure 2.

The tumoral volumes used for optimization of the tube in terms of limit of detection, uncertainty and exposure were 1-6 cm^3. The depths considered for the tumors were 1-3 cm (measured from the surface of the phantom to the surface of the tumors).

The improvements in absolute detection efficiency, which offer the LE-Ge detector, compared to the CdTe detector typically reported for this purpose (Gräfe et al., 2011; Almalki et al., 2010), are hampered by a loss in the spectral resolution. To compensate this effect, detection geometry was analyzed and optimized to better reduce the contribution of the Compton in the fluorescent signal region of Gd and avoid overlaps of both signals. The geometry used consisted of positioning the source and detector so that their normal vectors were at an angle of 90°, fixing the source at 45° and the detector at -45° with respect to the normal of the phantom used to evaluate the method.

2.4 Comparizon with ^{241}Am sources and calibration curve for quantification applications.

For the setup studied in the simulation, exposure calculation was performed using equation 2, considering the attenuation values in air of the NIST (Hubbell and Seltzer, 2004), taking the values of energy and particle flux of the exported file in each X-ray tube simulated. The exposure calculation is performed in order to have a parameter for comparison between the simulated X-ray tube and the ^{241}Am. Two different sources of ^{241}Am were simulated for the comparison with the optimized X-ray tube, for gadolinium quantification, using the gamma photons of 59.54 keV emitting with a 35.7% per decay rate. The activity of the first source was defined accordingly in order to consider generating an equal exposure to that produced by the optimized x-ray tube, so as to compare the advantages of the proposed method with similar reported in the literature (Almalki, 2010). One factor that affects the ability to properly assess improvements produced by the proposed method is the adding Cu filters in the configuration of the tube. This filter decreases the contribution to the exposure of photons with energies lower than the absorption edge (<50 keV). On the other hand, for the first ^{241}Am source, the percentage of exposure that contributes to photons with energies less than 50 keV, is 89.7%. Thus, it was necessary to define a second ^{241}Am source with a filter system, for decreases the contribution of energy that does not produce fluorescence and to reduce the contribution to exposure by this spectral region. Considering the attenuation coefficients for aluminium (Hubbell and Seltzer, 2004) at the energy range produced by the ^{241}Am spectrum, it was determined - based on Equation 2 - the reduction of the fraction to the exposure of the source to get a similar value obtained to the optimized X-ray tube. This filter enabled to define the second ^{241}Am source with a higher activity which the first source, but with a similar total exposure, increasing the efficiency in the production of fluorescent photons and allowing a better limit of detection.

The depths for the Gd quantification study in function of the tumor size are shown in Table 2.

Two cases were considered for the tumor distance: first, fixing the distance source-surface-of-the-tumor (tumors at 3 cm of depth) and second, keeping the distance source-center-of-the-tumor fixed (tumors at 1.2 to 3 cm of depth).

3. Results and discussion

The configuration of each X-ray beam described above allows a scanning energy from the absorption edge to the maximum energy allowed by the tube. The spectra used in the first stage have the same spectral width, but with different intensities, given the different thicknesses of the filter required to tune each energy and spectral shape of the Bremsstrahlung of a conventional tube. From the corresponding simulations, characteristic fluorescent spectra with background contributions given mainly by Compton scattering is obtained.

The qualitative differences between the number of fluorescent counts and the level of background around the peak of interest can be seen in Figure 3 for a specific tumor of 1 cm^3 at 3 cm of depth, indicating the feasibility of finding an optimal excitation energy between the two variables. From the quantitative analysis of the spectra obtained, a minimum in the limit of detection and the uncertainty can be observed (Figure 4) for an excitation spectrum with a central energy around 58.0±0.1 keV. The existence of a minimum was previously explained in similar application (detection of Kb of gold nanoparticles) (Figueroa et al., 2015) as follows: when the central energy of the incident spectrum is shifted from the absorption edge energy to higher values, the increment in the number of fluorescent photons increases more strongly than does the increase in background level produced by the shift of the Compton Peak towards the area of interest, using like criteria the limit of detection and the uncertainty (values at left side of the minimum in the curve of Figure 4). However, for values higher than which specific threshold energy, the shift of the Compton Peak begins an overlap with the studied fluorescence line, thus decreasing accuracy of the spectral identification (values in the right side of the minimum in the curve of figure 4). The minimum limit of detection can be observed (see Figure 5) for the same incident spectrum (58 keV) in a range of sizes (1 to 6 cm^3) and deep (1.2 to 3 cm) tumor, similar results those to obtained in the search for optimal incident spectra for the detection of gold nanoparticles (Figueroa et al., 2015).

The second stage of simulations made it possible to simultaneously evaluate the dependence between the limit of detection and the exposure produced by spectra of different widths (FWHM), centered on the determined optimum energy (58keV). The results are shown in Figure 6, which illustrates that for a desired limit of detection value, a configuration with a width at half height (FWHM) of 9.4±0.1 keV will produce a lower exposure, thus optimizing the system in terms of the dose that would be provided to the tissue, in their clinical applications. This would allow for setting different optimized sources to achieve a limit of detection to detect a signal of interest, along with the ability to define arbitrary the levels for the absorbed dose that will be for imaging. Similarly, it may be also possible to implement criteria focused on dose maximization, as may be useful for therapeutic purposes (functionalized nanoparticles as targeting agents).

In order to compare the results obtained by the optimized tube regarding sources with monochromatic spectral lines such as ^{241}Am isotope, the exposure value in air produced by the tube during the defined time of measurement was determined by Equation 2. This resulted in total exposure of $8.6x10^{-2}$ R, where the contribution by the spectral region less than 50 keV (absorption edge) was of 12.19% and by spectral region with the energy needed to produce fluorescence was of 87.81%. This

exposure obtained is equivalent to a dose delivery on the surface of the skin 0.79 mGy (considering a conversion factors of dose in soft tissue = 1.06 dose in air, and a conversion factors of exposure to dose for air f(air) = 0.869). This delivered dose is far below the maximum limit of 10 mGy recommended by *in vivo* X-ray techniques (Wielopolski, 1999).

From that total exposure value of the X-ray tube it was determined that an ^{241}Am source of 11.2 Ci of activity will produce the same exposure, if implemented with the same experimental geometries and time of measurement. For the same total exposure value and the respective percentage of contribution of the spectral region above and below the absorption edge (50 keV) obtained for the X-ray source, it was determined by the Eq. 2 that the second ^{241}Am source will have an activity of 169.8 Ci with a filter of 4.3 mm of Aluminum. The comparison of the results produced by ^{241}Am sources and the optimized X-ray tube for the determination of Gd in tumoral tissue, in terms of limit of detection and uncertainties, are shown in Table 3.

Using the X-ray tube whose peak is centered at 58 keV, two calibration curves were made. The results of the simulations are presented in Figures 7 and 8, which plot the number of Gd net counts detected in function of the size of each tumor. The curves for the first figure correspond to the peak located at 42.99 keV $K\alpha_1$, while the last figure corresponds to the net counts of the $K\alpha_2$ peak located at 42.31 keV.

The figures show a high linearity in the number of counts based on tumor size for both $K\alpha_1$ and $K\alpha_2$ lines in the case of maintaining fixed distance from the center of the tumor with an R^2 of 0.99 (Figure 5). This is because, at first approach, the tumor grows concentrically around the fixed point corresponding to the distance from the center of the tumor. However, in the other case, a non-linearity is observed because the tumor is inserted into the phantom as it grows, increasing the distance between the source-center tumor, which consequently increases with the distance between the center of the tumor and the detector. That is why the incident X-rays and fluorescent photons produced in the center of the tumor are attenuated by increased soft tissue around them, which consequently increases with increasing tumor size. This does not occur in the above. In addition, a linear correspondence in both methodologies is observed until it reaches a tumor size of 1.5 cm. At this point, the behavior shown in Figure 8 begins to decrease, by observing the aforementioned characteristic effect of X-ray attenuation.

4. Conclusions

An efficient system for *in vivo* detection of Gd has been configured using Monte Carlo simulations, based on the tuning of the kVp and the adding of filters of varying thickness to a conventional Radiology tube. The system is optimized to emit a spectrally narrow beam around 58 keV and 9.2 keV of FWHM, achieving low detection limit and uncertainties with minimum exposure. The results, when standardized in function of the exposure, are superior to those obtained by X-ray tube without optimized configuration and the radioactive Am-241 sources for these purposes, reported in the literature.

The results demonstred that the optimized X-ray tube achieves improvements greater than 5.7 times below detection limit and improvements below the uncertainties greater than 4.9 times compared with the first ^{241}Am source, and improvements of up to 2.3 times over the second ^{241}Am source. Those results show that the methodology provides the configuration of an incident spectrum that optimizes the detection of Gd in contrast with traditionally implemented methodologies.

The skin doses estimated for the system are found at 0.79 mGy, which is significantly below the maximum value recommended for *in vivo* XRF applications (10 mGy). Additionally, short time required

for measurement (16 s), would allow for the assessment of their future applications to determine spatial distributions of Gd.

The implementation of the configured system, in quantification applications, was evaluated for different tumor configurations doped with Gd, in order to assess the sensitivity of the system in different future clinical applications. The results show that sufficient signal is obtained to implement quantifications in the recommended therapeutic range (250 ppm) in tumors of 1-6 cm^3 at surface-surface-of-tumor depths of up to 3 cm in measurement time of only 16 s, remarking the high sensitivity of the studied system.

Acknowledgements

This work has been supported by the program CONICYT through the grant FONDECYT N°11150673 and by the Research Division of the Universidad de La Frontera, DIUFRO DI 14-6006. M. Vasquez thanks to CONICYT for the scholarship support Nº 22152075.

Reference

Almalki, M., Majid, S.A., Butler, P.H., Reinisch, L., 2010. Australas Phys Eng Sci Med. 33, 185-191.

De Stasio, G., Capozi, M., Lorusso, G.F., Baudat, P.A., Droubay, T.C., Perfetti, P., Margaritondo, G., Tonner, B.P., 1998. Rev. Instrum. 69, 2062-2067.

Dewi, N., Yanagie, H., Zhu, H., Demachi, K., Shinohara, A., Yokoyama, K., Sekino, M., Sakurai, Y., Morishita, Y., Iyomoto, N., Nagasaki, T., Horiguchi, Y., Nagasaki, Y., Nakajima, J., Ono, M., Kakimi, K., Takahashi, H., 2013. Biomedicine y Pharmacotherapy. 67, 451–457.

Enger, S.A., Giusti, V., Fortin, M.A, Lundqvist, H., af Rosenschöld, P.M., 2013. Radiation Measurements, 59, 233e240.

Figueroa, R., García, M., 2004. Radiation Physics and Chemistry. 71, 701–703.

Figueroa, R.G., Santibañez, M., Malano, F., Valente, M., 2015. Radiation Physics and Chemistry. 117, 198-202.

Fujimoto, T., Ichikawa, H., Akisue, T., Fujita, I., Kishimoto, K., Hara, H., Imabori, M., Kawamitsu, H., Sharma, P., Brown, S.C., Moudgil, B.M., Fujii, M., Yamamoto, T., Kurosaka, M., Fukumori, Y., 2009. Applied Radiation and Isotopes. 67, S355–S358.

Gräfe, J.L., McNeill, F.E., Byun, S.H., Chettle, D.R., Noseworthy, M.D., 2011. Applied Radiation and Isotopes. 69, 105-111.

Gräfe, J.L., 2012. *In Vivo* Detection Of Gadolinium By Prompt Gamma Neutron Activation Analysis: An Investigation Of The Potential Toxicity Of Gadolinium-Based Contrast Agents Used In MRI. A Thesis Submitted to the School of Graduate Studies in Partial Fulfilment of the Requirements for the Degree Doctor of Philosophy, McMaster University.

Hubbell, J.H., Seltzer, S.M., 2004. *Tables of X-Ray Mass Attenuation Coefficients and Mass Energy-Absorption Coefficients* (version 1.4). National Institute of Standards and Technology, Gaithersburg, MD.

ICRU (1980). Radiation quantities and units. Report 33, International Commission on Radiation Units and Measurements, 7910 Woodmont Ave., Bethesda, M D 20814.

Jenkins, R., Gould, R.W., Gedcke, D., 1981. Quantitative X-ray Spectrometry (Marcel Dekker, New York).

Le, U.M., Cui, Z., 2006. International Journal of Pharmaceutics. 320, 96–103.

Santibáñez, M., Bennun, L., Marcó-Parra, L.M., 2013. X-Ray Spectrom, 42, 442-449.

Salt, C., Lennox, A.J., Takagaki, M., Maguire, J.A., Hosmane, N.S., 2004. Russian Chemical Bulletin, International Edition. 53, 1871-1888.

Schoonjans, T., Vincze, L., Solé, V.A., Sanchez del Rio, M., Brondeel, P., Silversmit, G., Appel, K., Ferrero, C., 2012. Spectrochimica Acta Part B. 70, 10-23.

Schoonjans, T., Vincze, L., Solé, V.A., Sanchez del Rio, M., Appel, K., Ferrero, C., 2013. Spectrochimica Acta Part B. 82, 36-41.

Shih, J.L., Brugger, R.M., 1992. Med. Phys. 19, 733-734.

Van Grieken R., Markowicz, A., 2002. Handbook of X-ray Spectrometry, 2nd ed. (Marcel Dekker, New York).

Vincze, L., Janssens, K., Adams, F., 1993. Spectrochimica Acta Part B. 48, 553-573.

Vincze, L., Janssens, K., Vekemans B., Adams, F., 1999. Spectrochimica Acta Part B. 54, 1711-1722.

Wielopolski, L., 1999. Adv. X-Ray Anal. 41, 892–897.

Configuration for different central energy			Configuration for different FWHM		
Central Peak (keV)	kVp	Cu Filter (*mm*)	Spectrum width	*kV*p	Cu Filter (*mm*)
50.0±0.1	54.6	1.70	8.3±0.1	62	3.30
52.0±0.1	56.6	2.00	8.7±0.1	62.2	3.20
54.0±0.1	58.6	2.20	9.0±0.1	62.3	3.10
56.0±0.1	60.6	2.50	9.1±0.1	62.5	3.00
57.0±0.1	61.6	2.70	9.4±0.1	62.6	2.90
58.0±0.1	62.6	2.90	9.6±0.1	62.8	2.85
59.0±0.1	63.6	3.20	9.7±0.1	62.9	2.80
60.0±0.1	64.6	3.50	9.9±0.1	63	2.75
62.0±0.1	66.6	3.80	10.3±0.1	63.3	2.60
64.0±0.1	68.6	4.30	12.5±0.1	64.6	2.10
66.0±0.1	70.6	4.80	17.2±0.1	68.2	1.44
68.0±0.1	72.6	5.50	21.5±0.1	72.1	1.10
70.0±0.1	74.6	6.00	29±0.1	80.6	0.78

Table 1. Parameter of the different X-ray tubes simulated for producing different configuration of spectrum incident.

Configuration for a fixed center-tumor-to-source distance		Configuration for a fixed surface-tumor-to-source distance	
Tumoral size (cm^3)	Depth of the surface of the tumor (*cm*)	Tumoral size (cm^3)	Depth of the center of the tumor (*cm*)
1	3.0	1	3.0
2	2.6	2	3.0
3	2.3	3	3.0
4	1.9	4	3.0
5	1.6	5	3.0
6	1.2	6	3.0

Table 2. Tumoral dimensions and tissue thickness for the different configurations of tumor depth.

X-ray Tube / Am source	$K\alpha_1$		$K\alpha_2$	
	Limit of detection	Uncertainty	Limit of detection	Uncertainty
58.0 $\pm$0.1*keV*	29 ppm	5.5 %	56 ppm	10 %
11.2 *Ci* ^{241}Am	143 ppm	27 %	N/D	N/D
169.8 *Ci* ^{241}Am (with 4.3 *mm* Al)	68 ppm	13 %	60 ppm	11 %

Tabla 3. Comparison of the sensitivity obtained in different configurations: X-ray tube and the ^{241}Am source..

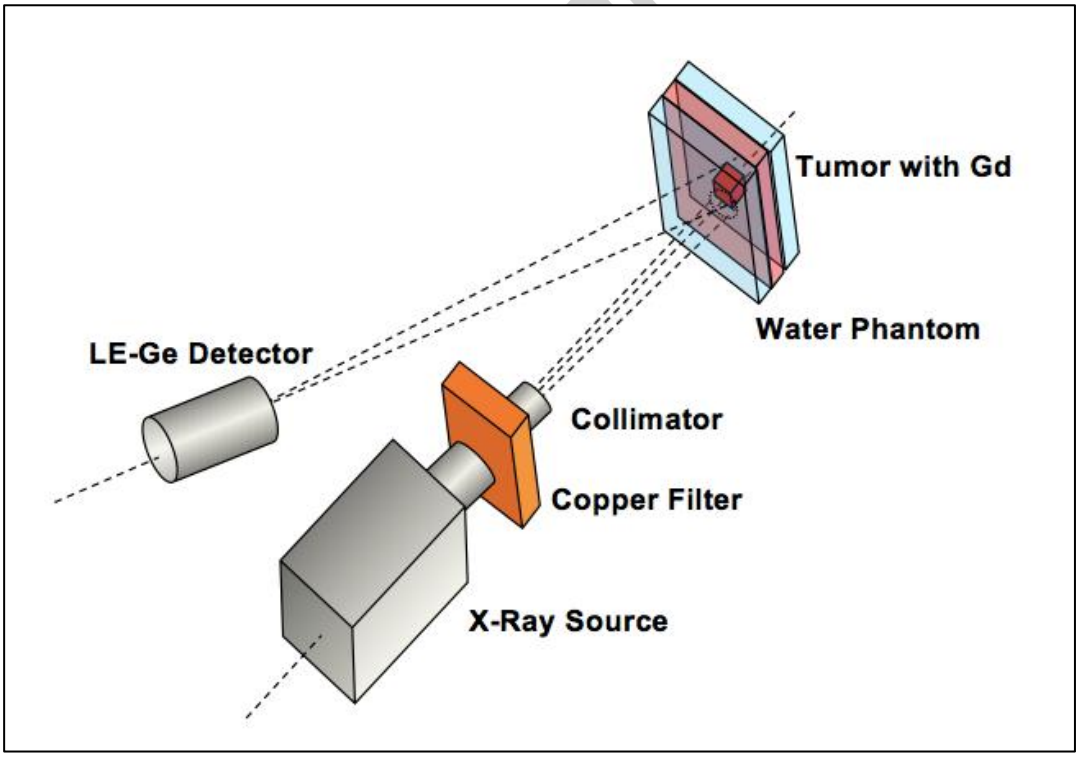

Fig. 1. Geometry of the proposed setup simulated by the XMI-MSIM code.

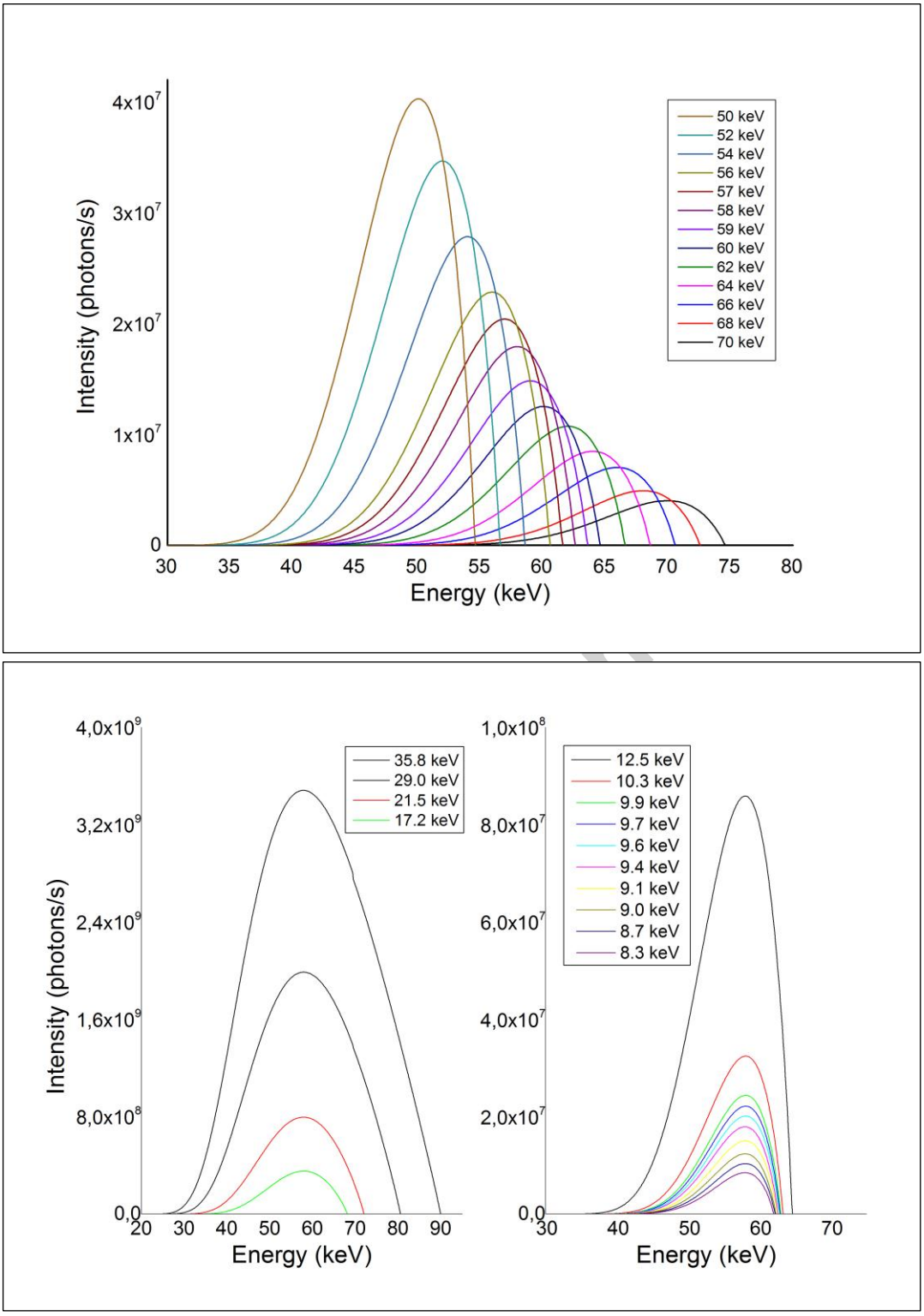

Fig. 2. Incident spectra with: a) Different central energy and the same spectral width, b) Different FWHM with the same central energy.

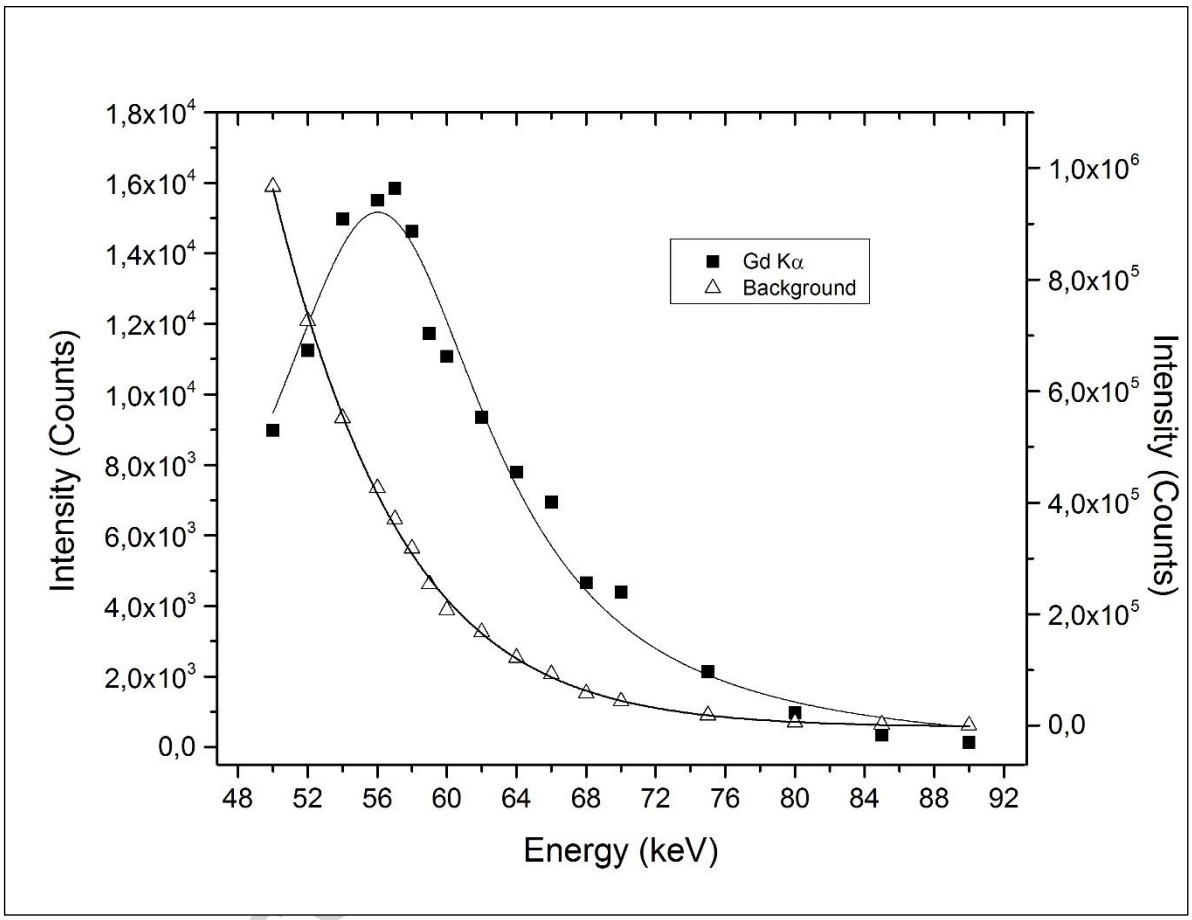

Fig. 3. Detected signal for fluorescent and background photons according to the central energy of the incident spectrum. Statistical errors less than 2%

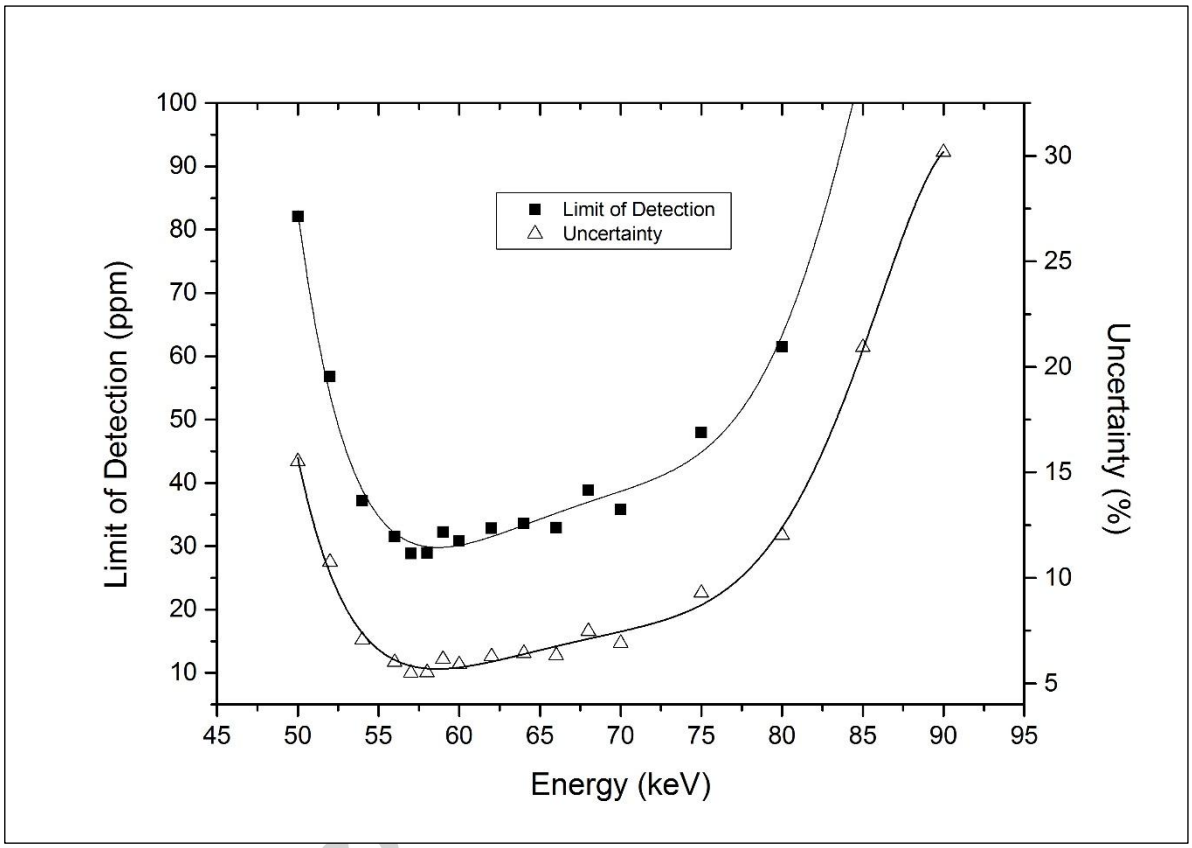

Fig. 4. Limit of detection and uncertainty obtained for the Gd $K\alpha_1$ peak in function of the central energy of the incent spectrum. Statistical errors less than 2%

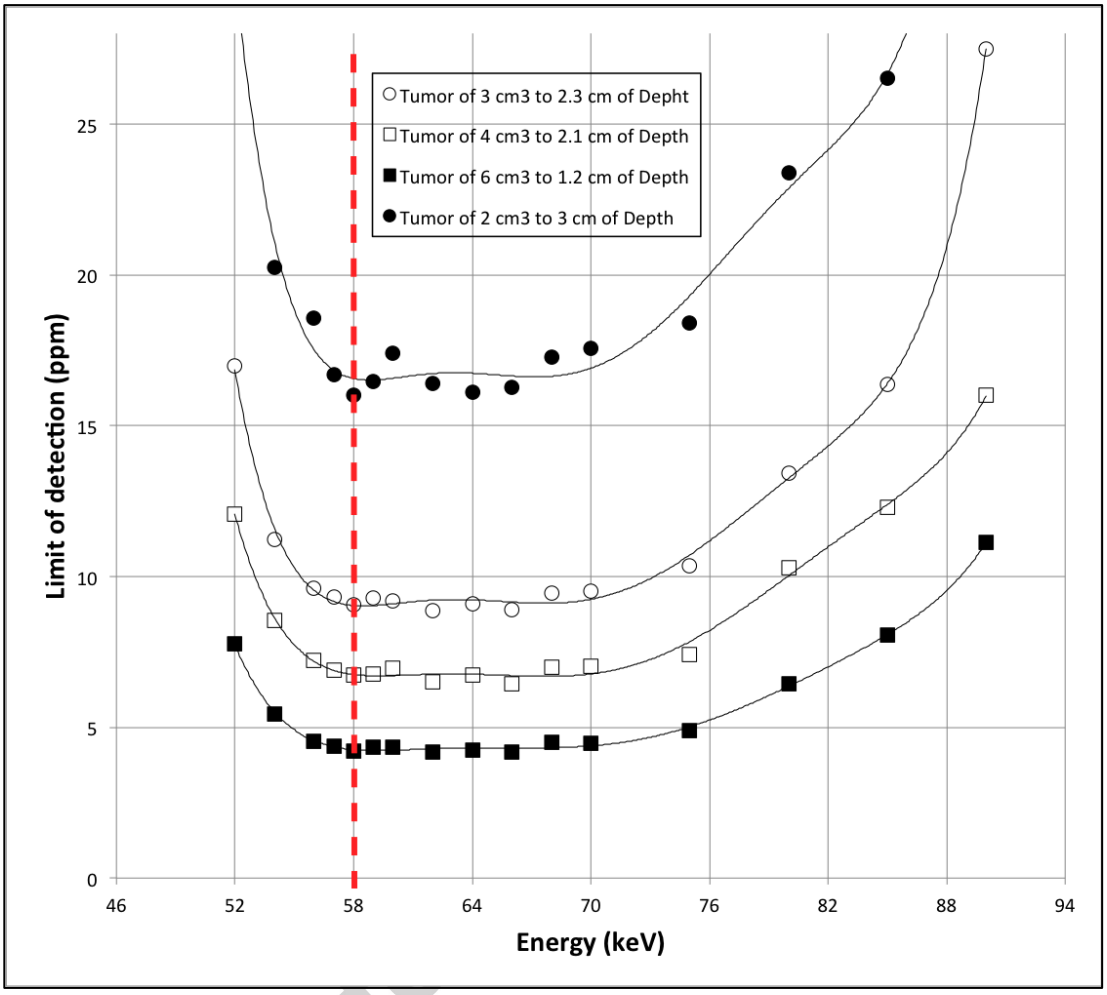

Fig. 5. Limit of detection for tumors of different sizes and different depths, obtained for the Gd $K\alpha_1$ peak in function of the central energy of the incent spectrum.

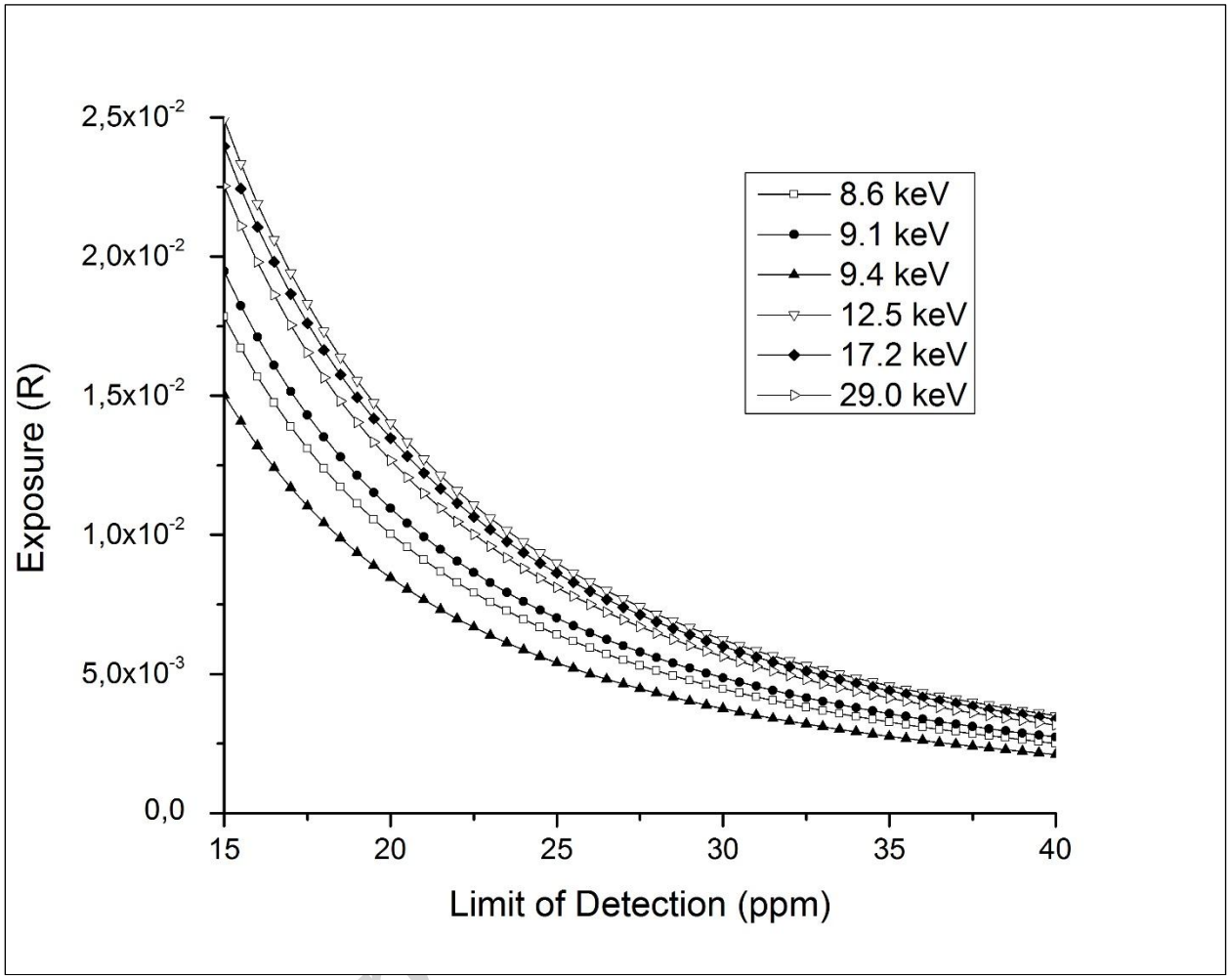

Fig. 6. Limit of detection and the exposure produced by spectra of different widths (FWHM), centered on the determined optimal energy.

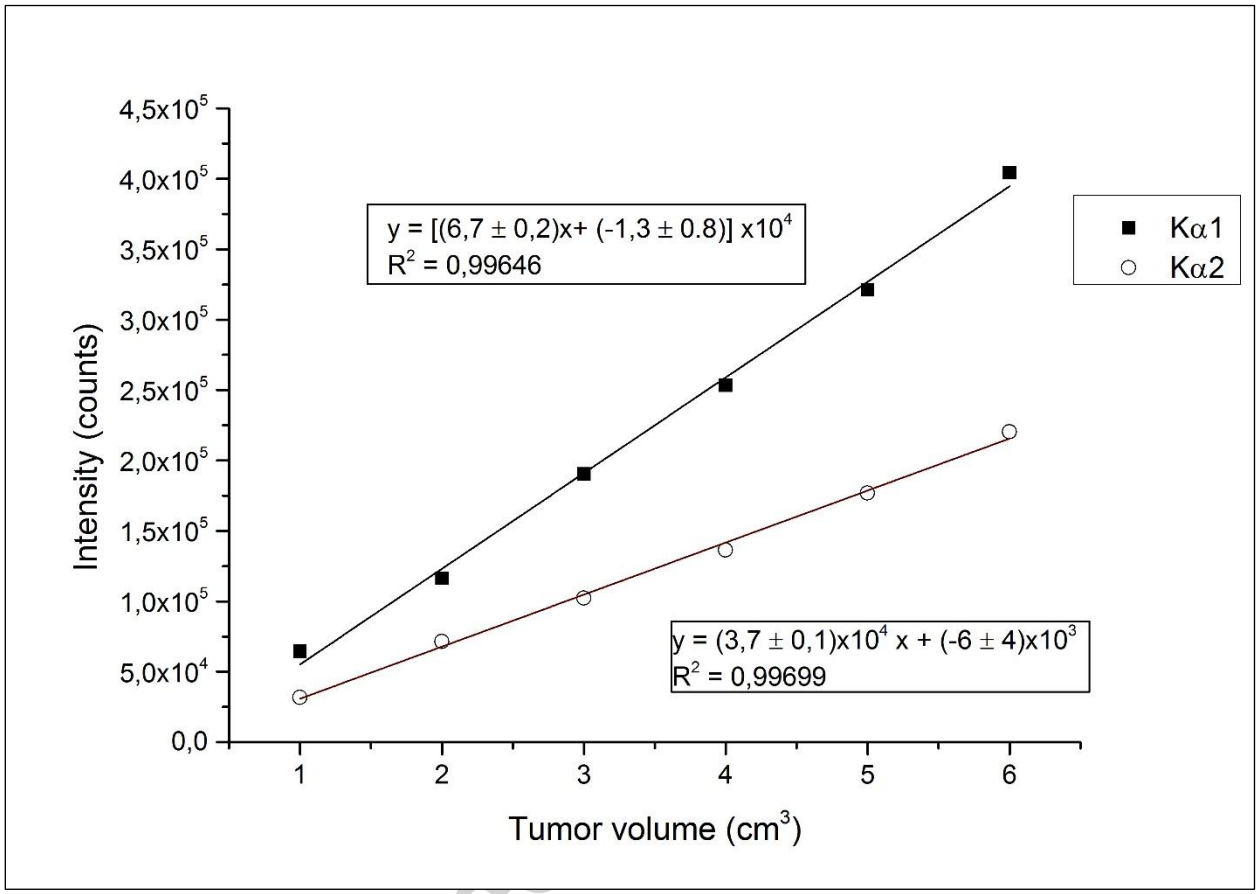

Fig 7. Calibration curves of peak intensity of Gd Kα2 and Kα1 in function of the tumor volume for a fixed center-tumor-source distance.

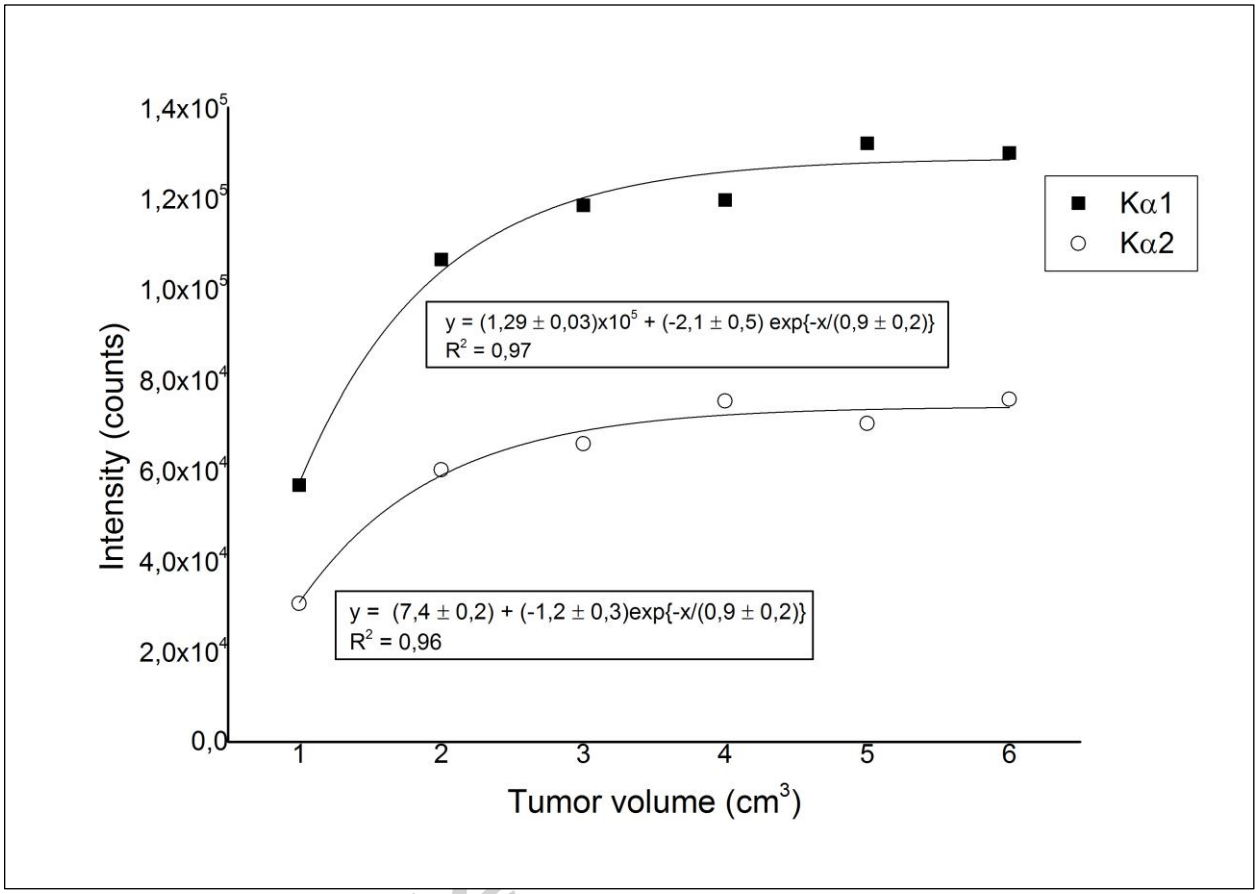

Fig. 8. Calibration curves of peak intensity of Gd Kα2 and Kα1 in function of the tumor volume for a fixed surface-tumor-source distance.

Highlights:

- Monte Carlo simulation achieving optimal EDXRF configuration for *in-vivo* biomedical application
- Determination of Gadolinium accumulation for contrast imaging and targeting radiotherapy
- Sensitivity improvement conditioned to minimum radiation exposure for future application in 2D chemical imaging of Gd.